MATURATION OF BRUSHITE ($CaHPO_4 \cdot 2H_2O$) AND *IN SITU* CRYSTALLIZATION OF BRUSHITE MICRO-GRANULES

Matthew A. Miller[1], Matthew R. Kendall[1], Manoj K. Jain[2], Preston R. Larson[3], Andrew S. Madden[1] and A. Cuneyt Tas[4]

[1] School of Geology and Geophysics, University of Oklahoma, Norman, OK 73019, USA
[2] College of Dentistry, University of Oklahoma Health Sciences Center, Oklahoma City, OK 73117, USA
[3] Samuel Roberts Noble Electron Microscopy Laboratory, University of Oklahoma, Norman, OK 73019, USA
[4] Department of Materials Science and Engineering, University of Illinois, Urbana, IL 61801, USA

ABSTRACT

Conventional flat plate (FP)-shaped brushite (DCPD, dicalcium phosphate dihydrate, $CaHPO_4 \cdot 2H_2O$), produced by reacting Ca-chloride and alkali phosphate salt solutions, were discovered to undergo a maturation process (changing their Ca/P molar ratio from 0.8 to the theoretical value of 1) similar to those seen in biological apatites. Water lily (WL)-shaped brushite crystals were produced in non-stirred aqueous solutions at room temperature in 24 hours by using precipitated calcite and $NH_4H_2PO_4$ as the starting chemicals. The hydrothermal transformation of WL-type brushite into octacalcium phosphate (OCP) or Ca-deficient hydroxyapatite (CDHA) was tested at 37°C by using four different biomineralization solutions, including Tris-buffered SBF (synthetic body fluid) and sodium lactate-buffered SBF solutions. All four solutions used in this study consumed the starting brushite in one week and caused transformation into a biphasic mixture of nanocrystalline OCP and CDHA of high surface area. WL-type brushite crystals when synthesized in the presence of small amounts of Zn^{2+} ions resulted in the formation of, for the first time, spherical micro-granules of brushite. Synthesis of brushite crystals in spherical morphology was not shown prior to this study.

INTRODUCTION

Brushite (DCPD, dicalcium phosphate dihydrate, $CaHPO_4 \cdot 2H_2O$), named after the American mineralogist George Jarvis Brush (1831-1912), is the predominant phase of the CaO-P_2O_5-H_2O system to precipitate between pH 2 and 6.5 [1-3], when Ca^{2+} and HPO_4^{2-} ions are brought together in an aqueous solution of this pH range. Brushite is mainly encountered in dental calculi, urinary stones and in chondrocalcinosis. It has a high solubility (pK_{SP} of 6.59 at 25°C) in comparison to the mineral of bone and teeth, hydroxyapatite, HA, $Ca_{10}(PO_4)_6(OH)_2$ (pK_{SP} of 116.8 at 25°C) [4]. Its solubility is also significantly higher than that of octacalcium phosphate, OCP, $Ca_8(HPO_4)_2(PO_4)_4 \cdot 5H_2O$ (pK_{SP} of 96.6 at 25°C) [4].

Brushite is stable over the pH range of 2 to 6.5, whereas OCP is stable from 5.5 to 7, and stoichiometric HA containing hydroxyl (OH^-) ions is stable over the neutral and basic pH range. Accordingly, brushite easily hydrolyzes to the more stable phases of OCP and apatite under physiological conditions [5, 6]. Brushite powders reacted with an aqueous solution containing NaOH (or KOH), for instance, transforms to apatite within minutes [7]. The transformation of apatite into brushite was also studied [8]. The literature on the synthesis of brushite seems to be abundant, however, it focuses largely on the reaction of Ca^{2+} ions originating from highly soluble salts of Ca-chloride, Ca-nitrate or Ca-acetate with the aqueous HPO_4^{2-} ions (from ammonium- or alkali-phosphate salts). The encounter between the above ions causes instantaneous precipitation

of flat plate (FP)- or lath-like crystals approximately 10 to 150 μm in length and 0.1 to 0.4 μm in thickness, depending on the solution's degree of supersaturation, pH, temperature and level of agitation [9, 10]. Alternatively, reaction of phosphate ions with precipitated $CaCO_3$ powder was previously shown to produce brushite with water lily (WL) or dumbbell morphology [11].

High solubility of brushite, in comparison to apatite, led to the development of injectable paste formulations based on brushite [12-14] with β-TCP (β-tricalcium phosphate, β-$Ca_3(PO_4)_2$) as the starting material. Apelt *et al.* [15] reported in a comparative *in vivo* study that the TCP-containing brushite cements were rapidly bio-degraded by macrophage activity and showed faster new bone formation compared to commercially available apatite cements. Therefore, the literature suggested that the *in vivo* degradability of future scaffolds based on brushite could be higher than those based on non-degradable apatite.

Studies on the *in vitro*, acellular testing of brushite in synthetic biomineralization or calcification solutions, such as SBF (simulated/synthetic body fluid [16, 17]) have been scarce [11, 18-26]. While some of those [18-23] examined the transformation of brushite observed in electrochemically deposited calcium- phosphates on titanium or in aqueous nucleation/crystallization on organic scaffolds, only a few of them [24-26] attempted studying pure brushite soaked in biomineralization solutions. The hydrothermal transformation of brushite powders having flat plate (FP)-type crystals was previously studied, at 37°C, in Tris-SBF solutions [24]. A recent study by Boccaccini *et al.* [27] disclosed that the Tris-buffer present in the conventional SBF solutions was able to cause an increased dissolution of the surface constituents of soaked bioglass and glass-ceramics samples and, therefore, led to the premature crystallization of apatite on sample surfaces, largely interfering with the reliability of the so-called bioactivity measurements performed in such SBF solutions.

Moreover, research on the synthesis of brushite in aqueous media containing biologically significant elements (such as zinc) was also quite limited [3, 6, 28-31]. Zinc is found in the body in small amounts in almost all tissues, however, the bones and teeth store slightly higher amounts than others. Human blood plasma also contains approximately 1.5×10^{-2} mM zinc [32]. Zinc is an essential trace element in a variety of cellular processes including DNA synthesis, behavioral responses, reproduction and virility, bone formation, bone growth and wound healing [33]. The necessity of this trace element for bone growth was demonstrated by the observation that normal bone growth was retarded in animals that are zinc-deficient [34], and the addition of zinc to these deficient diets resulted in the stimulation of both bone growth and biomineralization [35]. Research literature related to brushite synthesized in the presence of zinc is hard to come by.

The current study was designed to find answers to the following questions.

(1) Would brushite powders with the WL morphology soaked at 37°C (a) in Tris-buffered SBF solutions [36], (b) in lactic acid/Na-lactate buffered SBF solutions [37], or (c) in synthetic biomineralization media [26] mimicking the electrolyte portion of one of the most common cell culture solutions (*i.e.*, DMEM, Dulbecco's Modified Eagle Medium) display different or similar transformation products?

(2) How would Zn^{2+} ions added at small concentrations to the WL-type brushite synthesis solutions affect the morphology of the obtained brushite crystals?

EXPERIMENTAL

The starting chemicals of $CaCO_3$ (*calcite*, Fisher Scientific, Catalog No: C-63), $NH_4H_2PO_4$ (Fisher, No: A-684), $NaH_2PO_4 \cdot H_2O$ (Merck, No: SX-0710), $CaCl_2 \cdot 2H_2O$ (Fisher, No: C-79), $ZnCl_2$ (Merck, No: ZX-0065), $MgCl_2 \cdot 6H_2O$ (Fisher, No: AC-19753), NaCl (Sigma, No: S9888), KCl (Sigma, No: P3911), Na_2SO_4 (Fisher, No: AC-21875), $NaHCO_3$ (Fisher, No: S233),

Na_2HPO_4 (Fisher, No: S374), KH_2PO_4, $NaCH_3CH(OH)COO$ (Sigma, No: L7... tris(hydroxymethyl)aminomethane ($(HOC...$ study. Biomimetic testing and crystallizat... by using freshly prepared deionized water.

The procedure used to synthesize... preparing two solutions [11, 24]. Solution... dissolved in 700 mL of deionized water. Solution B was prepared by dissolving 4... was then rapidly added to solution A and t... or 24 h at room temperature (RT, 22±1°C)... by filtration (and follow-up washing with... are not included in Table 1.

Table I Sample preparation

Sample	Water (*mL*)	$NH_4H_2PO_4$ (*g*)	Na...
1	85	10.00	
2	85	—	
3	84.5	10.00	
4	84	10.00	
5	83	10.00	
6	82.5	10.00	
7	82	10.00	
8	81	10.00	

Water lily (WL) brushite was pr... $NH_4H_2PO_4$, equal to 8.6936×10^{-2} moles P, ... coated fish) in 85 mL of deionized water... addition of 2.0 g of $CaCO_3$ as calcite (1.9... this study is also known as the precipitated... toothpaste formulations. The bottle was scr... only a few minutes to facilitate the compl... phosphate solution. The bottle was then le... were separated from their mother liquor by... mL of water and dried at 37°C, overnight. ... the influence of ammonium ions on the m... (of Table 1) was prepared by using 11.9... 8.6936×10^{-2} mole of P.

To synthesize brushite crystals in the... similar to the above, we first prepared a stu... $ZnCl_2$ in 100 mL of deionized water). In this... were added to the above synthesis solution... preparation conditions for the select sampl... Table 1. The nominal Zn^{2+} (from the $ZnCl_2$... was given in the last column of Table 1. Effe... and the morphology of the brushite crystal... (Olympus, IX-71, Tokyo, Japan).

Na_2HPO_4 (Fisher, No: S374), KH_2PO_4 (Sigma, No: P0662), HCl (VWR, No: VW3110), $NaCH_3CH(OH)COO$ (Sigma, No: L7022), lactic acid (1 M, Fluka, No: 35202), and tris(hydroxymethyl)aminomethane ($(HOCH_2)_3CNH_2$, Sigma, No: 252859) were used in this study. Biomimetic testing and crystallization experiments were performed in clean glass bottles by using freshly prepared deionized water (18.2 MΩ).

The procedure used to synthesize flat-plate (FP)-shaped brushite crystals consisted of preparing two solutions [11, 24]. Solution A was prepared as follows: 0.825 g of KH_2PO_4 was dissolved in 700 mL of deionized water, followed by the addition of 3.013 g of Na_2HPO_4. Solution B was prepared by dissolving 4.014 g of $CaCl_2 \cdot 2H_2O$ in 200 mL of water. Solution B was then rapidly added to solution A and the precipitates formed were aged for either 80 min, 4 h or 24 h at room temperature (RT, 22±1°C), by continuous stirring at 300 rpm. Solids recovered by filtration (and follow-up washing with water) were dried overnight at 37°C. These samples are not included in Table 1.

Table 1 Sample preparation

Sample	Water (*mL*)	$NH_4H_2PO_4$ (*g*)	$NaH_2PO_4 \cdot H_2O$ (*g*)	$CaCO_3$ (*g*)	$ZnCl_2$ sol^n (*mL*)	Zn/Ca molar ratio
1	85	10.00	—	2.00	—	—
2	85	—	11.997	2.00	—	—
3	84.5	10.00		2.00	0.05	1.836×10^{-3}
4	84	10.00	—	2.00	1	3.672×10^{-3}
5	83	10.00	—	2.00	2	7.343×10^{-3}
6	82.5	10.00	—	2.00	2.5	9.179×10^{-3}
7	82	10.00	—	2.00	3	1.101×10^{-2}
8	81	10.00	—	2.00	4	1.469×10^{-2}

Water lily (WL) brushite was produced with a different procedure. Ten grams of $NH_4H_2PO_4$, equal to 8.6936×10^{-2} moles P, was dissolved (by stirring with a magnetic Teflon-coated fish) in 85 mL of deionized water in a 125 mL-capacity glass bottle, followed by the addition of 2.0 g of $CaCO_3$ as calcite (1.9983×10^{-2} moles Ca^{2+}) powder. The calcite powder of this study is also known as the precipitated $CaCO_3$ or precipitated chalk, which is also used in toothpaste formulations. The bottle was screw capped and the formed suspension was shaken for only a few minutes to facilitate the complete soaking of the $CaCO_3$ particle surfaces with the phosphate solution. The bottle was then kept perfectly static for 24 h at RT. WL-type crystals were separated from their mother liquor by filtration (Whatman No. 4 paper), washed with 300 mL of water and dried at 37°C, overnight. These are labeled as Sample-1 in Table 1. To check the influence of ammonium ions on the morphology of crystals obtained in sample-1, sample-2 (of Table 1) was prepared by using 11.997 g of $NaH_2PO_4 \cdot H_2O$, which was again equal to 8.6936×10^{-2} mole of P.

To synthesize brushite crystals in the presence of aqueous Zn^{2+} ions in static suspensions similar to the above, we first prepared a stock solution of $ZnCl_2$ dissolved in water (*i.e.*, 1.00 g $ZnCl_2$ in 100 mL of deionized water). In this study, 0.5 to 6 mL aliquots of this Zn stock solution were added to the above synthesis solutions which used $CaCO_3$ as the calcium source. The preparation conditions for the select samples of the brushite crystallization study are given in Table 1. The nominal Zn^{2+} (from the $ZnCl_2$ solution added) to Ca^{2+} (from $CaCO_3$) molar ratio was given in the last column of Table 1. Each crystallization run was repeated at least three times and the morphology of the brushite crystals was monitored by using an optical microscope (Olympus, IX-71, Tokyo, Japan).

Four different biomineralization solutions were used in this study [38], whose compositions are given in Table 2. The numbers in Table 2 denoted the amounts of chemicals added (in grams, except otherwise indicated) to 1 L of water to prepare the solutions. These solutions were stored in 1 L-capacity clean glass bottles in a refrigerator (+4°C) when they were not in use. All four solutions had a pH value of 7.4 when prepared, similar to the electrolyte portion of blood plasma. BM-7 [26], 27 mM-HCO_3-*Tris*-SBF [17, 36], and *Lac*-SBF [37] had a Ca/P molar ratio of 2.50, whereas the BM-3 [26] solution had a Ca/P molar ratio of 1.99 similar to that of DMEM (*Dulbecco's Modified Eagle Medium*) solutions. *Lac*-SBF solution perfectly matches the ion concentrations of blood plasma.

Table II Biomineralization solutions developed by our laboratory

Chemical	BM-3 [26]	BM-7 [26]	*Lac*-SBF [37]	*Tris*-SBF [17, 36]
NaCl	4.7865	4.7865	5.2599	6.5456
KCl	0.3975	0.3975	0.3730	0.3730
$MgCl_2 \cdot 6H_2O$	0.1655	0.1655	0.3049	0.3049
$CaCl_2 \cdot 2H_2O$	0.2646	0.3330	0.3675	0.3675
$NaHCO_3$	3.7005	3.7005	2.2682	2.2682
$NaH_2PO_4 \cdot H_2O$	0.1250	0.1250	—	—
Na_2HPO_4	—	—	0.1419	0.1419
Na_2SO_4	—	—	0.0710	0.0710
Tris	—	—	—	6.0570
1 M HCl	—	—	—	40 mL
Na-lactate	—	—	2.4658	—
1 M lactic acid	—	—	1.5 mL	—
Ca/P molar ratio	*1.99*	*2.50*	*2.50*	*2.50*

The biomineralization solutions were used to monitor the phase changes to occur in the brushite powders. One gram portions of brushite powders were placed in a glass bottle, followed by adding 100 mL of the specific solution. The bottles were kept static in a 37°C oven. The solutions were totally replenished (with an unused solution) every 24 h. Solids recovered at the end of the specified aging times were filtered, washed with water and dried at 30°C.

Samples were characterized by scanning electron microscopy (SEM, JEOL JSM-840A, Tokyo, Japan), energy dispersive x-ray spectroscopy (EDXS, Kevex, Thermo Scientific (Scotts Valley, CA) detector with iXRF System interface + EDS2008 software, Houston, TX), surface area measurements (BET, Brunauer-Emmett-Teller, Quantachrome Nova 2000e, Boynton Beach, FL), and powder x-ray diffraction (XRD, Ultima IV, Rigaku, Tokyo, Japan). SEM and EDXS samples were sputter-coated with a thin layer of Au-Pd alloy prior to imaging. Surface areas of powder samples were determined by five-point BET analysis of the nitrogen adsorption isotherm obtained at -196°C after degassing overnight at 30°C (Quantachrome Nova 2000e, Boynton Beach, FL). Samples for XRD runs were first ground in a mortar by using a pestle. All the XRD scans (λ=1.5406 Å) were performed in variable slit mode, with an irradiated area of 17 mm^2, a receiving slit of 0.3 mm, and a divergence height limiting slit of 10 mm. The scan range for each XRD sample was from 4 to 40° 2θ, with a step size of 0.02° and a 3 s count time on a rotating specimen holder.

RESULTS AND DISCUSSION

This study originated from an unexp
conventional brushite crystals which w
Experimental section. Brushite crystals w
aging time in their mother liquors, i.e., t
converging to unity. The inset in Figure 1
molar ratio of brushite crystals as a fu
morphology [38] and XRD trace of the c
aging time, either 80 minutes, 4 h or 24 h
for 4 h at RT in their synthesis solutions w

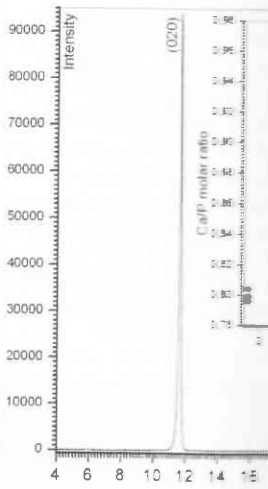

Figure 1. Maturation of brushite as a f

Such maturation processes are mor
the amorphous or cryptocrystalline (so cal
seen in new bone formation [39]. To the b
the maturation of brushite powder partic
crystal structure and these water layers ag
[40, 41]. Water molecules inside the crys
hydrogen bonds, but these hydrogen bon
were interrupted by the crystal surface ter
therefore hypothesize that the maturation
to the necessity of reaching a thermodyn
water bilayers to sandwich in between a si
to the brushite crystal structure. Since di
crystal, away from the surface) between t
ions, this may lead to an initial Ca-deficien
revealed this initial Ca-deficiency in brushi
an increase in the aging time in the mother

RESULTS AND DISCUSSION

This study originated from an unprecedented observation about the flat plate (FP)-shaped conventional brushite crystals which we synthesized according to the recipe given in the Experimental section. Brushite crystals went through a process of maturation as a function of aging time in their mother liquors, *i.e.*, their Ca/P molar ratio increased with time, eventually converging to unity. The inset in Figure 1 depicted the semi-quantitative EDXS-determined Ca/P molar ratio of brushite crystals as a function of time in the synthesis solution. The SEM morphology [38] and XRD trace of the crystals did not show any difference with respect to the aging time, either 80 minutes, 4 h or 24 h. The BET surface area of FP-brushite powders stirred for 4 h at RT in their synthesis solutions was measured to be 1.65 ± 0.1 m^2/g.

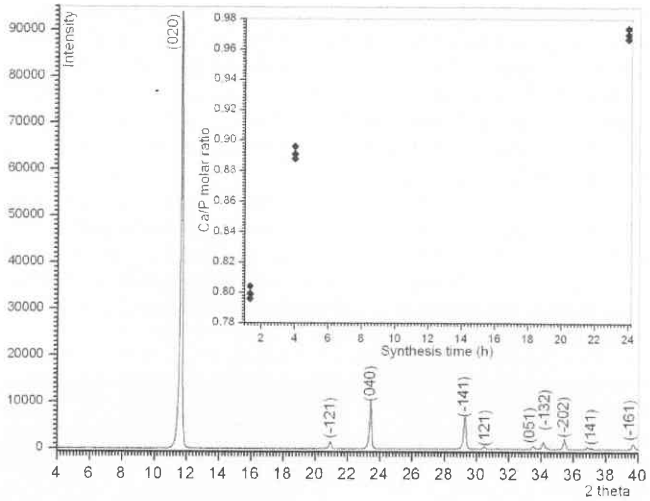

Figure 1. Maturation of brushite as a function of residence time in its synthesis solution

Such maturation processes are not uncommon in calcium phosphate phases, especially the amorphous or cryptocrystalline (so called poorly-crystalline) calcium phosphates/apatites, as seen in new bone formation [39]. To the best of our knowledge, this is the first study to report the maturation of brushite powder particles [38]. Brushite contains water incorporated in its crystal structure and these water layers appear as bilayers parallel to the (020) faces of crystals [40, 41]. Water molecules inside the crystal structure are linked to the HPO_4^{2-} groups by bulk hydrogen bonds, but these hydrogen bonds are broken when the bilayers of water molecules were interrupted by the crystal surface termination (as clearly shown in Fig. 1 of Ref. 40). We therefore hypothesize that the maturation phenomena exhibited by the brushite crystals was due to the necessity of reaching a thermodynamic equilibrium in the synthesis solutions for these water bilayers to sandwich in between a significant number of HPO_4^{2-} and Ca^{2+} ions, according to the brushite crystal structure. Since direct hydrogen bonds shall exist (in the bulk of the crystal, away from the surface) between the water bilayers and HPO_4^{2-} ions, but not with Ca^{2+} ions, this may lead to an initial Ca-deficiency in the formed crystals. The EDXS inset of Figure 1 revealed this initial Ca-deficiency in brushite for the first time, which drastically decreased with an increase in the aging time in the mother liquors.

Under the light of the above-mentioned observation, we slightly changed the way we planned to synthesize the brushite crystals to be used in the biomineralization solution testing part of this study. We had previously developed a new way of synthesizing water lily-shaped (instead of flat plate (FP)-shaped) brushite crystals [26] by reacting precipitated $CaCO_3$(s) in stirred aqueous solutions of $NH_4H_2PO_4$, however, in that previous study the formed crystals were separated from their mother solutions quite prematurely, after 30 minutes. Therefore, in the current study the time-of-stay in the mother solution was increased to 24 h. Each sample was checked for the Ca/P molar ratio by using EDXS. The FP-shaped brushite crystals (and their synthesis technique) were not used in this study after it provided the seed information.

Figures 2a and 2b showed the XRD trace and the SEM photomicrographs of sample-1 of Table 1, respectively. The water lily (WL)-shaped brushite crystals were about 100 μm in length and their XRD data conformed to the ICDD PDF 9-0077 standard pattern. One of the intense XRD peaks of water lily-type brushite is observed at 29.21° 2θ (Fig. 2a) and the major peak of calcite is expected to be seen at 29.41° 2θ (ICDD PDF 5-0586), which may be regarded as a close overlap. However, the next strong peak of calcite is located at 39.41° 2θ and this one does not pose an overlap with any of the peaks of the brushite phase. The low intensity peak detected at 39.4° 2θ in Fig. 2a could well correspond to the calcite phase, which accounts for the unreacted $CaCO_3$ in the static, non-agitated crystallization runs of this study.

The EDXS analysis performed on sample-1 yielded a Ca/P molar ratio of 0.98±0.03. This method of synthesizing brushite crystals always resulted in the reduction of the extraordinary intensity of the (020) reflection of FP-shaped brushite (as shown in Fig. 1a). WL-type brushite crystals are more intergrown, which helped to obtain a more disorientated distribution of smaller crystal plates and reduce the preferred orientation effects dominantly observed in the XRD spectra of FP-type brushite samples.

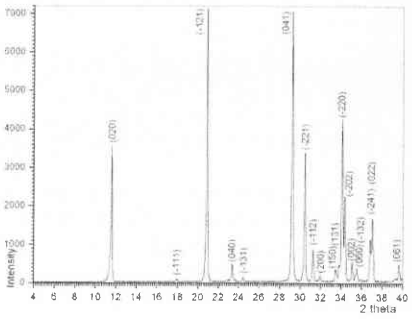

Figure 2a. XRD data of sample 1

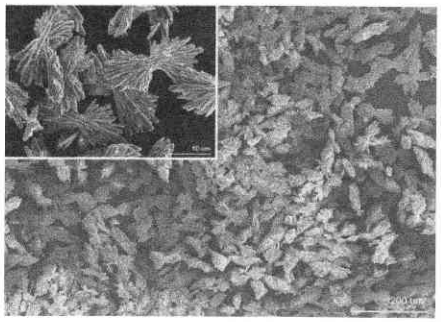

Figure 2b. SEM photos of sample 1

The BET surface area of sample-1 powders was found to be 0.37 m^2/g. Conventional FP-type brushite powders consisted of quite thin and fragile flat plates [38]. Such thin plates of brushite are not even resistant to the mechanical loads exerted during the spatula mixing of these FP powders together with other calcium phosphates, such as cryptocrystalline carbonated apatite or α-TCP powders in self-setting calcium phosphate bone cement applications. Water lily-type brushite powders (as in sample-1), in stark contrast to FP-type brushite, were found to retain their particle morphology even after light grinding with an agate pestle in an agate mortar. The smaller surface area of WL-type brushite (in comparison to that of FP) may also be beneficial for

the minimization of the volume of setting when such brushite powders are to be use of a bone cement or putty.

The following question arose at th 2b due to the ammonium ions in the $NH_4H_2PO_4$ was completely replaced by Na 2 of Table 1), by keeping the nominal Ca exactly the same. The answer was deci morphology (from conventional flat plates to those of the FP-shaped brushite synthe samples 1 and 2 were found to be identical with a greater ionic potential. If specific growing crystal significantly influenced have a greater effect. The lack of a noti served as spectator ions in the crystal morphology depicted in Figure 2b resemb deposition of brushite onto titanium or titan

The literature related to the testing [12-15] mentioned a slight inflammation implantation. This might be due to the rel major impetuses of the current study was account for this initial acidity of brushite, purpose, the WL-type powders of sample-1 physiological fluids or biomineralization s the acellular, inorganic electrolyte portion buffering agents, such as TRIS. The *in vitro* previously [24] in a 27 mM HCO_3^--TRIS-bu four different biomineralization solutions as time, and it was quite remarkable that all fo end of 2 days of soaking at 37°C. All four s solution pH from 3 to 7 days. It shall also [17, 36] and *Lac*-SBF [37] solutions were al

It should be noted that the *Tris*- and and sodium lactate-lactic acid pairs, respecti of soaking of the brushite powders at 37°C, are using the $HCO_3^-(aq)$-$CO_2(g)$ pair as the solution pH at 7.4 even during the first 24 acids and vitamins, closely resembles the i solutions, whereas the BM-7 solution is very ratio of 2.50 exactly matches that of human apparent advantage of not containing any or *etc.*) which the human blood does not have a

Figure 4 displays the powder XRD different time points, following drying at 30 mM-HCO_3^--TRIS-SBF and *Lac*-SBF was rec

the minimization of the volume of setting solution/liquid needed in bone cement applications, when such brushite powders are to be used as one of the constituents of the powder component of a bone cement or putty.

The following question arose at this point. Is this morphology of brushite shown in Fig. 2b due to the ammonium ions in the synthesis solutions? To answer that experimentally, $NH_4H_2PO_4$ was completely replaced by $NaH_2PO_4 \cdot H_2O$ in a number of experiments (*e.g.*, sample-2 of Table 1), by keeping the nominal Ca/P molar ratio in the solutions of sample-1 and sample-2 exactly the same. The answer was decisive; ammonium ions did not cause this change in morphology (from conventional flat plates (FP) to water lily, WL) and XRD data in comparison to those of the FP-shaped brushite synthesis practices [24]. The XRD and SEM data of both samples 1 and 2 were found to be identical. Na^+ is a large monovalent cation similar to NH_4^+, but with a greater ionic potential. If specific interactions between the monovalent cations and the growing crystal significantly influenced crystal growth, it would be expected that Na^+ would have a greater effect. The lack of a noticeable change illustrates that the monovalent cations served as spectator ions in the crystal growth process. Interestingly, the brushite crystal morphology depicted in Figure 2b resembled very much those obtained in the electrochemical deposition of brushite onto titanium or titanium alloy cathodes [42].

The literature related to the testing of the *in vivo* behavior of brushite-based bone cements [12-15] mentioned a slight inflammatory reaction observed within the first few days of implantation. This might be due to the release of acidic HPO_4^{2-} ions from brushite. One of the major impetuses of the current study was to search for *in vitro* testing procedures which could account for this initial acidity of brushite, without necessitating *in vivo* experimentation. To this purpose, the WL-type powders of sample-1 of this study were soaked in four different synthetic physiological fluids or biomineralization solutions (of Table 2) which were designed to mimic the acellular, inorganic electrolyte portion of blood plasma, with or without using organic buffering agents, such as TRIS. The *in vitro* testing of FP-type brushite powders were performed previously [24] in a 27 mM HCO_3-TRIS-buffered SBF. Figure 3 depicted the pH change in those four different biomineralization solutions as a function of brushite powder (WL, sample-1) aging time, and it was quite remarkable that all four solutions showed the minimum in pH value at the end of 2 days of soaking at 37°C. All four solutions then exhibited a gradual but constant rise in solution pH from 3 to 7 days. It shall also be noted here that BM-3 [26], BM-7 [26], *Tris*-SBF [17, 36] and *Lac*-SBF [37] solutions were all at pH 7.4 at the time of their preparation.

It should be noted that the *Tris*- and *Lac*-SBF solutions, which are buffered with Tris-HCl and sodium lactate-lactic acid pairs, respectively, did not exhibit a drop in solution pH after 24 h of soaking of the brushite powders at 37°C. On the other hand, BM-3 and BM-7 solutions, which are using the $HCO_3^-(aq)$-$CO_2(g)$ pair as the weak buffering agent, were not able to maintain the solution pH at 7.4 even during the first 24 h. BM-3 solution (Ca/P=1.99), devoid of any amino acids and vitamins, closely resembles the inorganic, electrolyte portion of DMEM cell culture solutions, whereas the BM-7 solution is very similar to the BM-3 solution except its Ca/P molar ratio of 2.50 exactly matches that of human blood [26]. BM-3 and BM-7 solutions do possess the apparent advantage of not containing any organic buffering agents (such as Tris, Hepes, lactate, *etc.*) which the human blood does not have as well.

Figure 4 displays the powder XRD data of samples recovered from BM-7 solutions, at different time points, following drying at 30°C. The direct comparison of BM-7 solution with 27 mM-HCO_3-TRIS-SBF and *Lac*-SBF was recently published elsewhere [38].

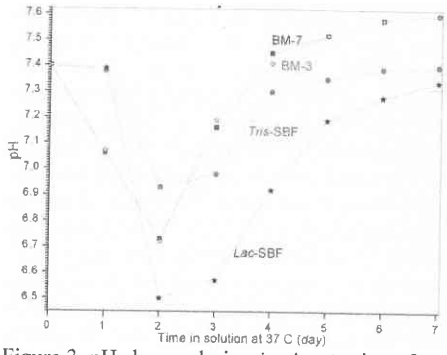

Figure 3. pH change during *in vitro* testing of sample-1

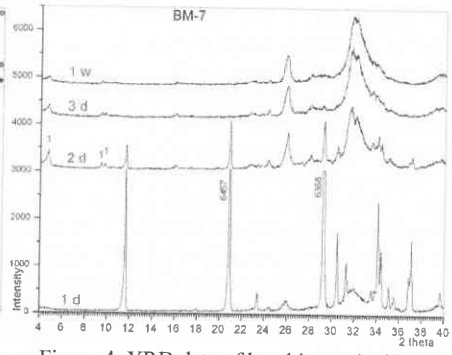

Figure 4. XRD data of brushite soaked in BM-7 solution at 37°C

The simultaneous observation of OCP ($Ca_8(HPO_4)_2(PO_4)_4 \cdot 5H_2O$, Ca/P molar=1.33) and CDHA (Ca-deficient hydroxyapatite, Ca/P molar=1.50) phases in the data of Fig. 4 can be explained by the below reactions.

$$10CaHPO_4 \cdot 2H_2O \rightarrow Ca_8(HPO_4)_2(PO_4)_4 \cdot 5H_2O + 2Ca^{2+} + 4H_2PO_4^- + 15H_2O \quad (1)$$

$$6CaHPO_4 \cdot 2H_2O + 2Ca^{2+} \rightarrow Ca_8(HPO_4)_2(PO_4)_4 \cdot 5H_2O + 4H^+ + 7H_2O \quad (2).$$

Equation (2) helps to explain the necessary presence of Ca^{2+} ions in the solutions in order to form OCP (Ca/P molar=1.333) from brushite (Ca/P molar=1.00). The transformation or hydrolysis of OCP into CDHA can be expressed by

$$Ca_8(HPO_4)_2(PO_4)_4 \cdot 5H_2O + Ca^{2+} \rightarrow Ca_9(HPO_4)(PO_4)_5(OH) + 2H^+ + 4H_2O \quad (3).$$

Protons generated in equation (3) would help to explain why all the solutions of Fig. 3 still struggled to raise the pH to the physiological level (7.4) by the 3rd day. The organic-free solutions BM-3 and BM-7 were able to raise the pH to the physiological level (7.4) at day 4.

All four solutions used in this study produced the same clear result; the presence of OCP in all the samples even after one week of soaking [38]. This result is quite strong in the sense that brushite first transforms into OCP in synthetic physiological solutions, and under the experimental conditions of this study, direct transformation of brushite into CDHA-like apatitic calcium phosphate, without first passing through the OCP phase, was not observed. OCP is long regarded as the precursor of bone mineral [43]. The SEM morphology of the brushite powders soaked in BM-3, BM-7, 27 mM-HCO_3-TRIS-SBF and *Lac*-SBF solutions (of Table 2) were reported elsewhere [38]. Brushite powders soaked in all the biomineralization media exhibited BET surface areas larger than 100 m^2/g [38].

Samples 3 through 8 of Table 2 were synthesized to investigate the influence of small concentrations of Zn^{2+} ions in the brushite synthesis solutions on the resultant crystal morphology. The nominal Zn/Ca solution molar ratios in these experiments were given in Table 2. EDXS analyses performed on these samples were not able to detect any Zn in the synthesized samples; ICP-AES would have been the better choice of analysis (instead of EDXS) to determine the much smaller amounts of Zn which might have been incorporated into these samples. However, the influence exerted on the crystal morphology of brushite by the Zn^{2+} ions present in the non-agitated, static synthesis solutions was drastic, as shown in the SEM micrographs given in Figure 5.

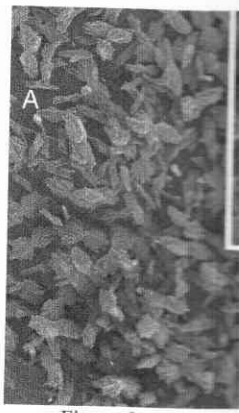

Figure 5a. SEM p

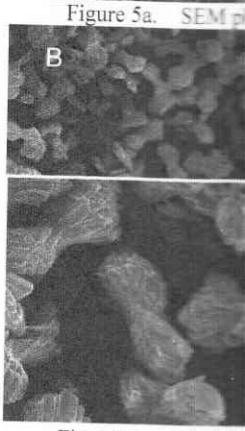

Figure 5b. SEM p

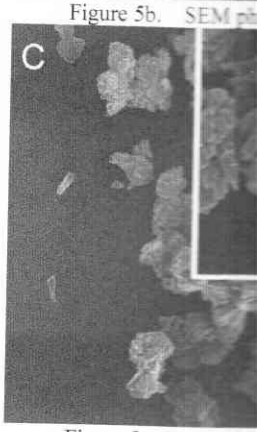

Figure 5c. SEM pho

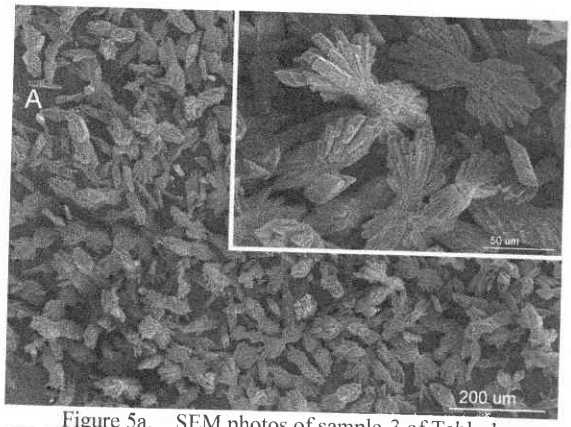

Figure 5a. SEM photos of sample-3 of Table 1

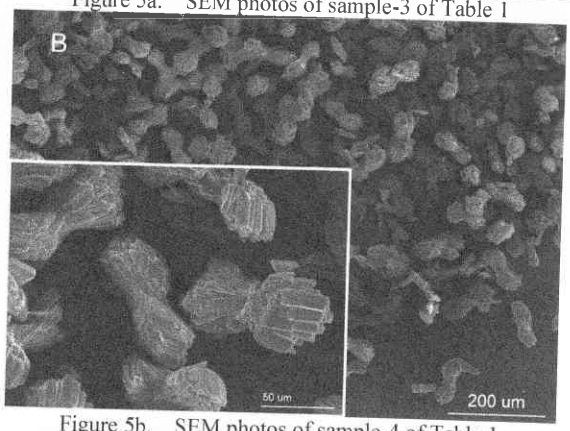

Figure 5b. SEM photos of sample-4 of Table 1

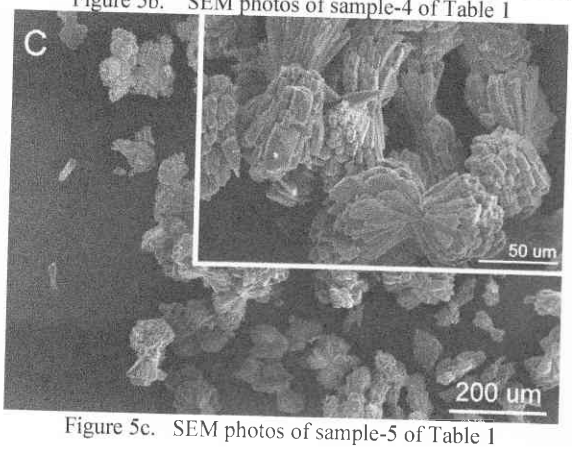

Figure 5c. SEM photos of sample-5 of Table 1

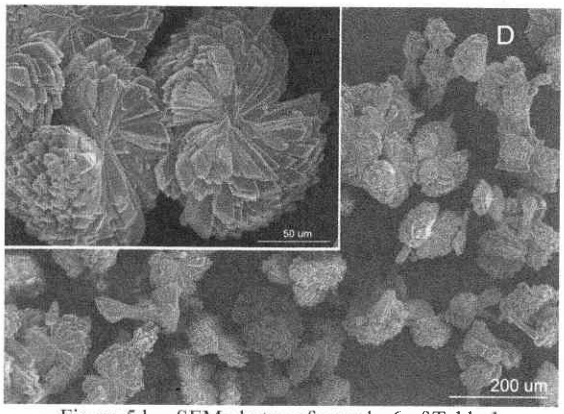

Figure 5d. SEM photos of sample-6 of Table 1

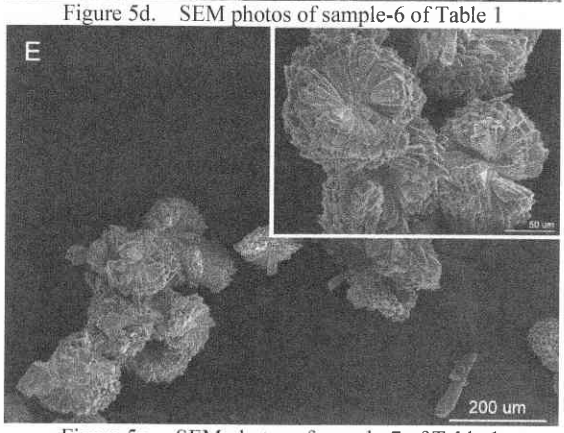

Figure 5e. SEM photos of sample-7 of Table 1

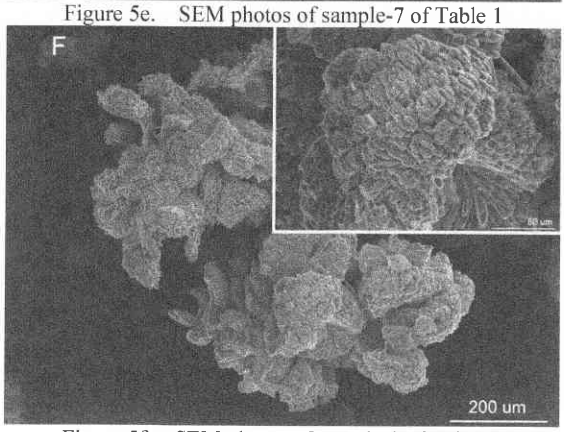

Figure 5f. SEM photos of sample-8 of Table 1

The lowest concentration of Zn us
the water lily-shaped brushite crystals to a
individual plates of the original water lily-
increase in the Zn concentration of the sy
caused the filling of the gaps between t
brushite were formed. Those dumbbells pr
in samples 6 through 8 (Figs. 5d through 5f
synthesis solutions. The mean granule size

XRD traces given in Fig. 6 show
(conforming to the ICDD PDF 9-0077) wit
similar to that shown in Fig. 2a for Zn-free

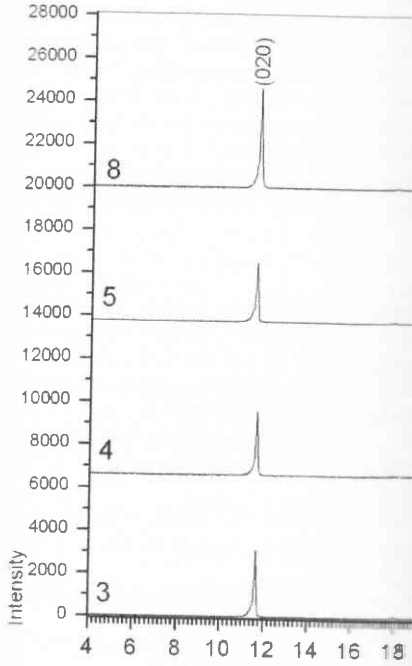

Figure 6. XRD data of brushite gran

Zinc phosphate ($Zn_3(PO_4)_2 \cdot nH_2O$) cem
century to join the tooth root to the crown.
amorphous zinc phosphate phase [44, 45].
highly crystalline material and can readily
of $ZnCl_2$ and ammonium phosphate. The X
hopeite (Fig. 6).

When we replaced Zn with Mg or Fe
samples 3 through 8), microgranules did not

The lowest concentration of Zn used during the synthesis of sample-3 (Fig. 5a) caused the water lily-shaped brushite crystals to acquire the dumbbell-shape, with the thickening of the individual plates of the original water lily-shape (in comparison to sample-1 of Fig. 2b). Further increase in the Zn concentration of the synthesis solutions (samples 4 and 5; Figs. 5b and 5c) caused the filling of the gaps between the individual plates and much denser dumbbells of brushite were formed. Those dumbbells progressively turned into more or less spherical granules in samples 6 through 8 (Figs. 5d through 5f), with further increase in the Zn concentration of the synthesis solutions. The mean granule size in samples 5 through 8 was around 100 μm.

XRD traces given in Fig. 6 showed that the phase of those granules was brushite (conforming to the ICDD PDF 9-0077) with a suppressed intensity of the (020) reflection, quite similar to that shown in Fig. 2a for Zn-free sample-1.

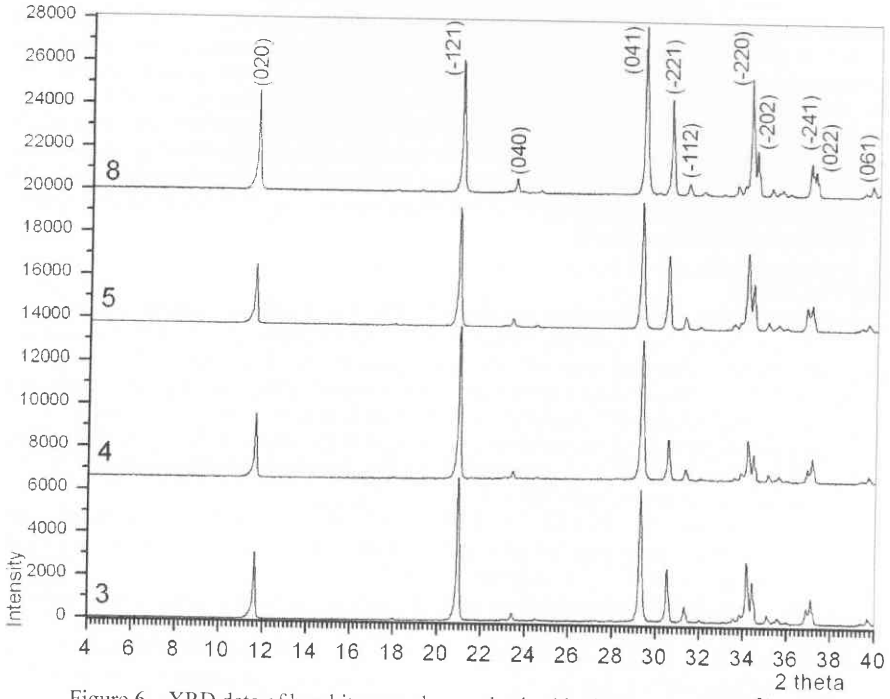

Figure 6. XRD data of brushite granules synthesized in the presence of Zn^{2+} ions

Zinc phosphate ($Zn_3(PO_4)_2 \cdot nH_2O$) cements have been used in dentistry since the late 19th century to join the tooth root to the crown, and the initial phase formed is an acidic and x-ray amorphous zinc phosphate phase [44, 45]. Hopeite ($Zn_3(PO_4)_2 \cdot 4H_2O$), on the other hand, is a highly crystalline material and can readily form in aqueous solutions containing dissolved salts of $ZnCl_2$ and ammonium phosphate. The XRD data of samples 3 through 8 did not show any hopeite (Fig. 6).

When we replaced Zn with Mg or Fe (under experimental conditions similar to those of samples 3 through 8), microgranules did not form, only WL-type brushite crystals were obtained.

When we added similar amounts of Zn^{2+} ions to the FP-synthesis recipes, such microgranules did not form as well.

Madsen [6] reported that the Zn ion has an inhibitory effect on the brushite crystallization along its (010) face and caused the crystallization of aggregated brushite crystals. Apparently, the presence of Zn ions in the synthesis solutions of this study were resulting in a gradual increase in the surface free energy of the individual platelets making up those thick water lily (Fig. 5a) and dumbbell-shaped brushite (Fig. 5b) crystals, and the system was responding to that increase in surface energy by decreasing the available surface area, *i.e.*, crystals acquiring the shape of spherical microgranules (Figs. 5d to 5f). These granules (initial BET surface area <1 m^2/g) soaked for 1 week in BM-7 solution (37°C) were found to have a post-soaking BET surface area of 30 m^2/g and largely transformed into an OCP-CDHA biphasic mixture.

It would be worthwhile to note that the syntheses described here were for static, non-agitated crystallization systems, free of any organic substances, and this would render this method of granule production, in the presence of Zn^{2+}, quite economical. Usually granulation processes for calcium phosphate bioceramics require the use of closely-controlled pelletizers and the simultaneous addition of certain benign organics and plasticizers to the initial powder mixtures. The complete removal of those organics may then pose a serious challenge to the engineer if the biomaterials are to be used in clinical implantation. Our follow-up study on the preparation of these granules will first focus on the determination of the ppm level incorporation of zinc into the resultant brushite granules. Such microgranules may find uses in the manufacture of biopolymer-brushite composites.

CONCLUSIONS

(1) Conventional, flat plate-type brushite crystals were shown to undergo a maturation process during their synthesis, meaning that their Ca/P molar increased from around 0.8 for 80 min of stay in the synthesis solution to around 1 for 24 h of stay in the same.

(2) Brushite crystals prepared at room temperature in static crystallization systems containing precipitated calcite and $NH_4H_2PO_4$ as the starting chemicals were found to transform into a biphasic mixture of octacalcium phosphate (OCP) and Ca-deficient hydroxyapatite (CDHA) when soaked for 1 week in different biomineralization solutions (including Tris- and sodium lactate-buffered SBF solutions) at 37°C.

(3) Biomineralization solution selected did not change the phase assemblage of the resultant material. Brushite crystals did not directly transform into single-phase apatite in 1 week of soaking time in any of the solutions used in this study.

(4) Static soaking of brushite crystals in different biomineralization media always resulted in a significant increase in the BET surface areas of the samples.

(5) The presence of small concentrations of Zn^{2+} ions in the brushite synthesis solutions dramatically changed the crystal morphology. Spherical microgranules of brushite were synthesized for the first time in non-agitated, organic-free aqueous systems.

ACKNOWLEDGEMENTS

M. K. Jain took part in this study as a
for a very limited time and we are hereby grat
Society through its Student Summer Resear
Jonathan Hill, Jeff Westrop, and Jordan W
measurements. During this study, A. C. Tas
University of Oklahoma Health Sciences Cent

REFERENCES

[1] P. W. Brown, Phase Relationships in
Ceram. Soc., **75**, 17-22 (1992).
[2] R. I. Martin and P. W. Brown, Phase
Ceram. Soc., **80**, 1263-6 (1997).
[3] E. Boanini, M. Gazzano, and A. Bigi, Ion
Low Temperature, *Acta Biomater.*, **6**, 1882
[4] S. V. Dorozhkin and M. Epple, Biologi
Angew. Chem. Int. Ed., **41**, 3130-46 (2002)
[5] H. Monma and T. Kamiya, Preparation
Mater. Sci., **22**, 4247-50 (1987).
[6] H. E. L. Madsen, Influence of Foreign
Brushite ($CaHPO_4 \cdot 2H_2O$) and Its Transf
Cryst. Growth, **310**, 2602-12 (2008).
[7] K. Furutaka, H. Monma, T. Okura, and S
System Brushite-NaOH Solution, *J. Eur. C*
[8] C. Oliveira, P. Georgieva, F. Rocha, A.
Brushite Precipitation, *J. Cryst. Growth*, **30**
[9] F. Abbona, F. Christensson, M. F. Ange
Conditions of Brushite, $CaHPO_4 \cdot 2H_2O$, *J. C*
[10] V. S. Joshi and M. J. Joshi, FTIR Spectr
of Calcium Hydrogen Phosphate Dihydrate
[11] S. Mandel and A. C. Tas, Brus
($Ca_8(HPO_4)_2(PO_4)_4 \cdot 5H_2O$) Transformation
30, 245-54 (2010).
[12] B. Flautre, C. Maynou, J. Lemaitre, P. va
TCP Granules incorporated in Brushite Cem
[13] J. M. Kuemmerle, A. Oberle, C. Oech
Rechenberg, Assessment of the Suitability
Cranioplasty – An Experimental Study in Sh
[14] F. Theiss, D. Apelt, B. Brand, A. Kutte
Auer, and B. von Rechenberg, Biocompatib
Cement, *Biomaterials*, **26**, 4383-94 (2005).
[15] D. Apelt, F. Theiss, A.O. El-Warrak, K.
Matter, J. A. Auer, and B. von Rechenbe
Hydraulic Calcium Phosphate Cements, *Bio*
[16] T. Kokubo, Surface Chemistry of Bioacti
(1990).
[17] D. Bayraktar and A. C. Tas, Chemical
Powders at 37°C in Urea-containing Synth
(1999).

ACKNOWLEDGEMENTS

M. K. Jain took part in this study as a summer student researcher of the OU College of Dentistry for a very limited time and we are hereby grateful to the financial support provided by J. Dean Robertson Society through its Student Summer Research Program. Authors gratefully acknowledge the help of Jonathan Hill, Jeff Westrop, and Jordan Williams (OU-Norman) for assistance with BET and XRD measurements. During this study, A. C. Tas was a visiting professor in the College of Dentistry of the University of Oklahoma Health Sciences Center (between September 2010 and September 2011).

REFERENCES

[1] P. W. Brown, Phase Relationships in the Ternary System $CaO-P_2O_5-H_2O$ at 25°C, *J. Am. Ceram. Soc.*, **75**, 17-22 (1992).

[2] R. I. Martin and P. W. Brown, Phase Equilibria among Acid Calcium Phosphates, *J. Am. Ceram. Soc.*, **80**, 1263-6 (1997).

[3] E. Boanini, M. Gazzano, and A. Bigi, Ionic Substitutions in Calcium Phosphates Synthesized at Low Temperature, *Acta Biomater.*, **6**, 1882-94 (2010).

[4] S. V. Dorozhkin and M. Epple, Biological and Medical Significance of Calcium Phosphates, *Angew. Chem. Int. Ed.*, **41**, 3130-46 (2002).

[5] H. Monma and T. Kamiya, Preparation of Hydroxyapatite by the Hydrolysis of Brushite, *J. Mater. Sci.*, **22**, 4247-50 (1987).

[6] H. E. L. Madsen, Influence of Foreign Metal Ions on Crystal Growth and Morphology of Brushite ($CaHPO_4 \cdot 2H_2O$) and Its Transformation to Octacalcium Phosphate and Apatite, *J. Cryst. Growth*, **310**, 2602-12 (2008).

[7] K. Furutaka, H. Monma, T. Okura, and S. Takahashi, Characteristic Reaction Processes in the System Brushite-NaOH Solution, *J. Eur. Ceram. Soc.*, **26**, 543-7 (2006).

[8] C. Oliveira, P. Georgieva, F. Rocha, A. Ferreira, and S. F. de Azevedo, Dynamical Model of Brushite Precipitation, *J. Cryst. Growth*, **305**, 201-10 (2007).

[9] F. Abbona, F. Christensson, M. F. Angela, and H. E. L. Madsen, Crystal Habit and Growth Conditions of Brushite, $CaHPO_4 \cdot 2H_2O$, *J. Cryst. Growth*, **131**, 331-46 (1993).

[10] V. S. Joshi and M. J. Joshi, FTIR Spectroscopic, Thermal and Growth Morphological Studies of Calcium Hydrogen Phosphate Dihydrate Crystals, *Cryst. Res. Technol.*, **38**, 817-21 (2003).

[11] S. Mandel and A. C. Tas, Brushite ($CaHPO_4 \cdot 2H_2O$) to Octacalcium Phosphate ($Ca_8(HPO_4)_2(PO_4)_4 \cdot 5H_2O$) Transformation in DMEM Solutions at 36.5°C, *Mater. Sci. Eng. C*, **30**, 245-54 (2010).

[12] B. Flautre, C. Maynou, J. Lemaitre, P. van Landuyt, and P. Hardouin, Bone-Colonization of β-TCP Granules incorporated in Brushite Cements, *J. Biomed. Mater. Res.*, **63B**, 413-7 (2002).

[13] J. M. Kuemmerle, A. Oberle, C. Oechslin, M. Bohner, C. Frei, I. Boecken, and B. von Rechenberg, Assessment of the Suitability of a New Brushite Calcium Phosphate Cement for Cranioplasty – An Experimental Study in Sheep, *J. Cranio Maxill. Surg.*, **33**, 37-44 (2005).

[14] F. Theiss, D. Apelt, B. Brand, A. Kutter, K. Zlinszky, M. Bohner, S. Matter, C. Frei, J. A. Auer, and B. von Rechenberg, Biocompatibility and Resorption of a Brushite Calcium Phosphate Cement, *Biomaterials*, **26**, 4383-94 (2005).

[15] D. Apelt, F. Theiss, A.O. El-Warrak, K. Zlinszky, R. Bettschart-Wolfisberger, M. Bohner, S. Matter, J. A. Auer, and B. von Rechenberg, In Vivo Behavior of Three Different Injectable Hydraulic Calcium Phosphate Cements, *Biomaterials*, **25**, 1439-51 (2004).

[16] T. Kokubo, Surface Chemistry of Bioactive Glass-Ceramics, *J. Non-Cryst. Solids*, **120**, 138-51 (1990).

[17] D. Bayraktar and A. C. Tas, Chemical Preparation of Carbonated Calcium Hydroxyapatite Powders at 37°C in Urea-containing Synthetic Body Fluids, *J. Eur. Ceram. Soc.*, **19**, 2573-9 (1999).

[18] R. R. Kumar and M. Wang, Biomimetic Deposition of Hydroxyapatite on Brushite Single Crystals grown by the Gel Technique, *Mater. Lett.*, **49**, 15-9 (2001).
[19] S. J. Lin, R. Z. LeGeros, and J. P. LeGeros, Adherent Octacalcium Phosphate Coating on Titanium Alloy using Modulated Electrochemical Deposition Method, *J. Biomed. Mater. Res.*, **66A**, 819-28 (2003).
[20] H.S. Azevedo, I. B. Leonor, C. M. Alves, and R. L. Reis, Incorporation of Proteins and Enzymes at Different Stages of the Preparation of Calcium Phosphate Coatings on a Degradable Substrate by a Biomimetic Methodology, *Mat. Sci. Eng. C*, **25**, 169-79 (2005).
[21] J. Pena, I. I. Barba, A. Martinez, and M. Vallet-Regi, New Method to obtain Chitosan/Apatite Materials at Room Temperature, *Solid State Sci.*, **8**, 513-9 (2006).
[22] F. Yang, J. G. C. Wolke, and J. A. Jansen, Biomimetic Calcium Phosphate Coating on Electrospun Poly(epsilon-caprolactone) Scaffolds for Bone Tissue Engineering, *Chem. Eng. J.*, **137**, 154-61 (2008).
[23] A. Rakngarm and Y. Mutoh, Electrochemical Deposition of Calcium Phosphate Film on Commercial Pure Titanium and Ti-6Al-4V in Two Types of Electrolyte at Room Temperature, *Mat. Sci. Eng. C*, **29**, 275-83 (2009).
[24] A. C. Tas and S. B. Bhaduri, Chemical Processing of $CaHPO_4 \cdot 2H_2O$: Its Conversion to Hydroxyapatite, *J. Am. Ceram. Soc.*, **87**, 2195-2200 (2004).
[25] J. A. Juhasz, S. M. Best, A. D. Auffret, and W. Bonfield, Biological Control of Apatite Growth in Simulated Body Fluid and Human Blood Serum, *J. Mater. Sci. Mater. M.*, **19**, 1823-9 (2008).
[26] N. Temizel, G. Girisken, and A. C. Tas, Accelerated Transformation of Brushite to Octacalcium Phosphate in New Biomineralization Media between 36.5° and 80°C, *Mat. Sci. Eng. C*, **31**, 1136-43 (2011).
[27] D. Rohanova, A. R. Boccaccini, D. M. Yunos, D. Horkavcova, I. Brezovska, and A. Helebrant, Tris Buffer in Simulated Body Fluid Distorts the Assessment of Glass-Ceramic Scaffold Bioactivity, *Acta Biomater.*, **7**, 2623-30 (2011).
[28] M. H. Salimi, J. C. Heughebaert, and G. H. Nancollas, Crystal Growth of Calcium Phosphates in the Presence of Magnesium Ions, *Langmuir*, **1**, 119-22 (1985).
[29] A. Bigi, M. Gazzano, A. Ripamonti, and N. Roveri, Effect of Foreign Ions on the Conversion of Brushite and Octacalcium Phosphate into Hydroxyapatite, *J. Inorg. Biochem.*, **32**, 251-7 (1988).
[30] P. N. Kumta, C. Sfeir, D. H. Lee, D. Olton, and D. Choi, Nanostructured Calcium Phosphates for Biomedical Applications: Novel Synthesis and Characterization, *Acta Biomater.*, **1**, 65-83 (2005).
[31] D. H. Lee and P. N. Kumta, Chemical Synthesis and Stabilization of Magnesium Substituted Brushite, *Mater. Sci. Eng. C*, **30**, 934-43 (2010).
[32] S. Cin, E. Unal, A. Pamir, B. Kologlu, and A. O. Cavdar, Blood Zinc (Plasma, Red Blood Cell) and Insulin-like Growth Factor-1 in Children from an Impoverished area in Ankara, *J. Trace Elem. Exp. Med.*, **14**, 31-4 (2001).
[33] D.G. Barceloux, Zinc, *J. Toxicol. Clin. Toxicol.* **37**, 279-92 (1999).
[34] G. Oner, B. Bhaumick, and R.M. Bala, Effect of Zinc-deficiency on Serum Somatomedin Levels and Skeletal Growth in Young Rats, *Endocrinology*, **114**, 1860-3 (1984).
[35] M. Yamaguchi, H. Oishi, and Y. Suketa, Stimulatory Effect of Zinc on Bone Formation in Tissue Culture, *Biochem. Pharmocol.*, **36**, 4007-12 (1987).
[36] A. C. Tas, Synthesis of Biomimetic Ca-Hydroxyapatite Powders at 37°C in Synthetic Body Fluids, *Biomaterials*, **21**, 1429-38 (2000).
[37] A. Pasinli, M. Yuksel, E. Celik, S. Sener, and A. C. Tas, A New Approach in Biomimetic Synthesis of Calcium Phosphate Coatings using Lactic Acid-Na Lactate Buffered Body Fluid Solution, *Acta Biomater.*, **6**, 2282-8 (2010).

[38] M. A. Miller, M. R. Kendall, M. K. Jain,
of Brushite ($CaHPO_4 \cdot 2H_2O$) in Synthetic Bi
of Brushite Micro-Granules, *J. Am. Ceram. S*
[39] S. Cazalbou, C. Combes, D. Eichert, C. R
Evolution and Maturation In Vitro and In Vi
[40] J. Arsic, D. Kaminski, P. Poodt, and E.
Interface, *Phys. Rev. B*, **69**, 245406 (2004).
[41] N. A. Curry and D. W. Jones, Cr
Orthophosphate Dihydrate: A Neutron Diff
Theor., **23**, 3725-9 (1971).
[42] J. Redepenning and J. P. McIsaac, Electr
Alloys, *Chem. Mater.*, **2**, 625-7 (1990).
[43] M. Iijima and Y. Moriwaki, Effects of Ion
Octacalcium Phosphate; Relevant to Tooth E
(1999).
[44] L. Herschke, J. Rottstegge, I. Lieberwir
Material for Potential Biomedical Applicatio
[45] L. Herschke, I. Lieberwirth, and G. Wegner
Biomedical Applications Part II, *J. Mater. Sci*

[38] M. A. Miller, M. R. Kendall, M. K. Jain, P. R. Larson, A. S. Madden, and A. C. Tas, Testing of Brushite ($CaHPO_4 \cdot 2H_2O$) in Synthetic Biomineralization Solutions and *In Situ* Crystallization of Brushite Micro-Granules, *J. Am. Ceram. Soc.*, **95**, 2178-2188 (2012).
[39] S. Cazalbou, C. Combes, D. Eichert, C. Rey, and M. J. Glimcher, Poorly Crystalline Apatites: Evolution and Maturation In Vitro and In Vivo, *J. Bone Miner. Metab.*, **22**, 310-17 (2004).
[40] J. Arsic, D. Kaminski, P. Poodt, and E. Vlieg, Liquid Ordering at the Brushite-010-Water Interface, *Phys. Rev. B*, **69**, 245406 (2004).
[41] N. A. Curry and D. W. Jones, Crystal Structure of Brushite, Calcium Hydrogen Orthophosphate Dihydrate: A Neutron Diffraction Investigation, *J. Chem. Soc. A-Inorg. Phys. Theor.*, **23**, 3725-9 (1971).
[42] J. Redepenning and J. P. McIsaac, Electrocrystallization of Brushite Coatings on Prosthetic Alloys, *Chem. Mater.*, **2**, 625-7 (1990).
[43] M. Iijima and Y. Moriwaki, Effects of Ionic Inflow and Organic Matrix on Crystal Growth of Octacalcium Phosphate; Relevant to Tooth Enamel Formation, *J. Cryst. Growth*, **198/199**, 670-6 (1999).
[44] L. Herschke, J. Rottstegge, I. Lieberwirth, and G. Wegner, Zinc Phosphate as Versatile Material for Potential Biomedical Applications Part I, *J. Mater. Sci. Mater. M.*, **17**, 81-94 (2006).
[45] L. Herschke, I. Lieberwirth, and G. Wegner, Zinc Phosphate as Versatile Material for Potential Biomedical Applications Part II, *J. Mater. Sci. Mater. M.*, **17**, 95-104 (2006).

Advances in Bioceramics and Porous Ceramics VI

Ceramic Engineering and Science Proceedings
Volume 34, Issue 6, 2013

Edited by
Roger Narayan
Paolo Colombo

Volume Editors
Soshu Kirihara and Sujanto Widjaja

The American Ceramic Society

WILEY

Cover Design: Wiley

Published by John Wiley & Sons, Inc., Hoboken, New Jersey.
Published simultaneously in Canada.

Library of Congress Cataloging-in-Publication Data is available.

ISBN: 978-1-118-80766-8
ISSN: 0196-6219

Printed in the United States of America.

10 9 8 7 6 5 4 3 2 1